Polar
Geophysical
Institute

THEMIS SPACE-GROUND OBSERVATIONS IN MIDNIGHT SECTOR DURING THE SUBSTORM RECOVERY PHASE

T.V. Kozelova, B.V. Kozelov *(Polar Geophysical Institute, Murmansk region, Russia)*

Abstract. We report a case study of substorm recovery phase on 14 November 2014 in the interval 20:30-23:00 UT using data from THEMIS-D satellite located in the midnight sector (~2300-0030 MLT) magnetosphere at 6.5-9.25 Re. The substorm recovery phase of interest was not just a decline of previous disturbances, but include also a new intense substorm intensification in the midnight sector of the auroral oval. This new auroral activation presents the eastward expanding auroral (EEA) structures occurred precisely after the substorm intensification onset and concentrated to the midnight sector of the auroral oval.

We show that these EEA structures were observed in diffuse aurora, formed the undulations on the poleward edge of the diffuse aurora similar to of omega bands. The pulsating aurora was observed after the passage of the EEA structures. Rapid poleward expansion of the poleward diffuse region boundary coincided with the occurrence of Pi2 pulsations in the ionosphere and with the large-scale dipolarization and the particle injections in the near-Eart plasma sheet of the magnetosphere at ~7.2 Re. Besides, the THEMIS-D reveals the quasiperiodic variations of electrostatic ELF wave intensity at frequency of <100 Hz coincided with the DC electric field variation. At the moments of more small-scale local dipolarizations, the low-energy electron flux (0.1-3 keV) bursts occur simultaneously with the ELF wave intensity enhancements.

1. Substorm evolution

The substorm of 14 November 2014 (Kp=3+) began near Amderma (AMD) at ~ 18:05 UT. The H=-500 nT was minimal at ~ 18:50 UT. After ~19 UT, during the substorm decay phase, the magnetic pulsations (30-40 min periodicity) in the Ps6 wave band were observed from AMD to Tromso (TRO). During this recovery phase in 20:30–22:30 UT interval, when the initial substorm expansive phase decreases, a new substorm disturbance initiated in the midnight sector.

In this paper we focus on the changes occur both in the ionosphere and in the magnetosphere in the midnight sector during this substorm decay phase in 20:30–22:30 UT interval, when three auroral substorm activations A1, A2 and A3 occur above the Kola Peninsula. We used the auroral data from Apatity all-sky camera and the data observed by the THEMIS-D satellite (THD). In this interval, the THD location changes from L=9.25 to L=6.5 and MLT from 23.9 to 0.5.

Activations A1 and A2. Fig.1 shows the map of ground-based stations, the projections of the auroras and the THD satellite footprints along magnetic field-line during the activation A1 at 21:15–21:40 UT. From this figure one can see that the auroral activity propagated westward from AMD to APT-LOZ-SOD and presents the weak auroral activity of pseudo-breakup type. Before the activation onset a weak azimuthal auroral arc was located in the APT zenith (21:09:30 UT), accompanied by auroral activity to the north. We analyze auroral activity occurring at most equatorward arc at the latitude ~ 67.7°. At the moment ~21:16 UT, the arc bifurcated, then its equatorward part moved to lower latitudes and northward part expanded to the north (to LOZ). The moment t_1=21:20 UT, when the Pi2-like pulsations of the magnetic field occur at the LOZ, was associated with the substorm activation A1 onset. After t_1 the *bulging form* of weak aurora appears at longitudes 28° – 36°. Western edge of this form reached the longitude 28° at ~ 21:33 UT. At ~21:36 UT, the northward border of the bulging auroral form has the maximum latitude (~ 68.7° at LOP). The auroral activity inside this weak bulging form has been neglected and then after ~21:36 UT, the western part of this auroral form quickly faded.

At the interval 21:45 – 21:55 UT new very weak auroral activity A2 occurs poleward the APT. The moment t_2=21:52 UT was the activation A2 onset. Other details of its development cannot be easily distinguished. This activity was classified also as weak auroral pseudo-breakup.

On the whole, one can say that during two initial activations A1 and A2 the small ground-based magnetic disturbances dH>0 were observed at the longitudes from AMD to AND and they were just a decline of previous disturbances, associated with the substorm near AMD at ~ 18:05 UT. During the activation A1, the footprints of the THD were mapped in the field of view of Apatity all-sky camera and were located northward equatorial-most arc. Before ~21:33 UT, the THD was located westward expanded bulging aurora and at ~ 21:33–21:36 UT the THD observed the passage of western edge of activation A1.

Activation A3. Fig. 2 shows the auroral dynamics during the activation A3 at 22:15–22:35 UT. A clear auroral arc appear from the west along the 67.8° latitude at ~22:20 UT. After 22:20 UT the auroral emission expanded northward and eastward over APT. The moment t_3 = 22:23 UT, when the Pi2-like pulsations of the magnetic field occur at the LOZ, was associated with the substorm activation A3 onset. This onset begins westward the APT (possibly near the AND-TRO) and was more intense than the A1 and A2. During the activation A3, more intense ground-based magnetic disturbances dH<0 were observed at the longitudes LOZ-AND, which associated with intensified westward auroral electrojet.
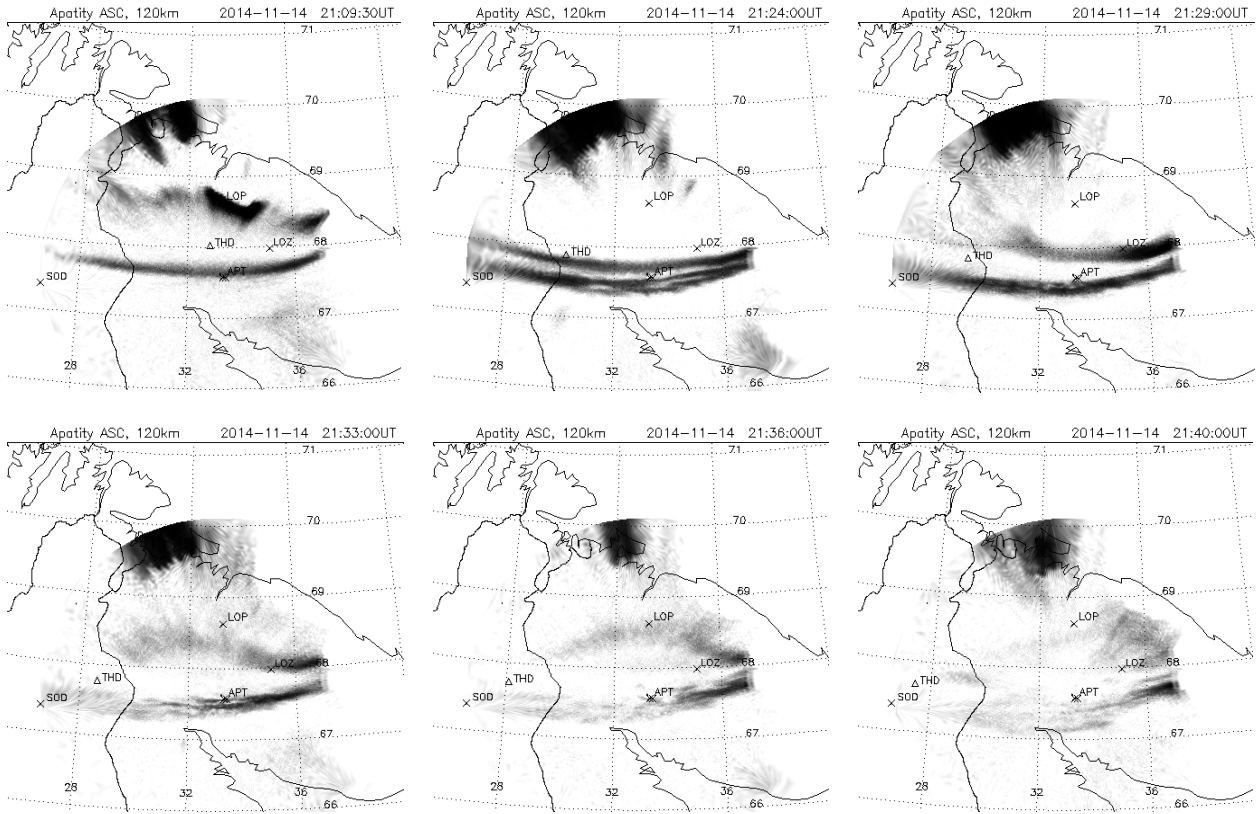
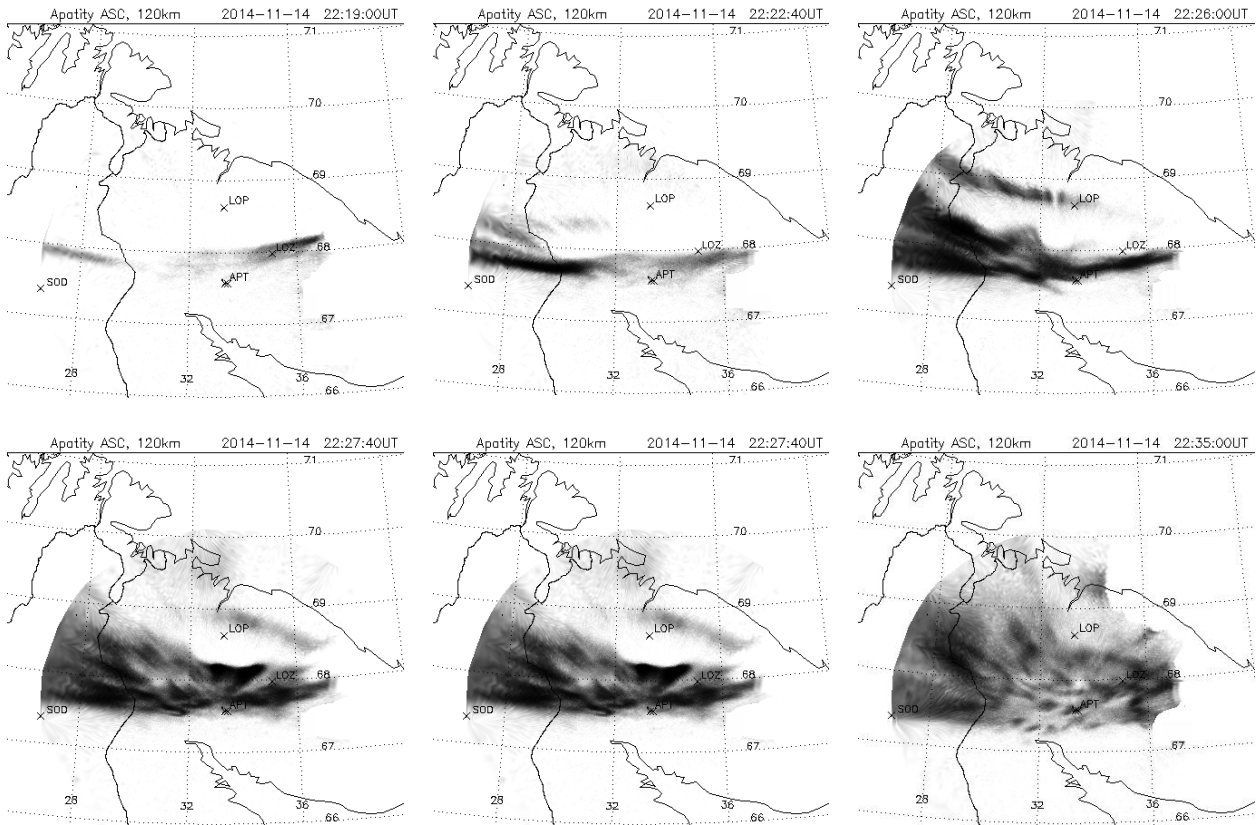**Figure 1.** Auroras at Apatity all-sky camera during first activation A1 on Nov 14, 2014.


Figure 2. Auroras at Apatity all-sky camera during the third activation A3 on Nov 14, 2014.

At ~22:26 UT the auroral surge (patch-like) appears near the 68° and the 32° longitude, which brightened and propagated eastward along the poleward border of the diffuse aurora. At the interval 22:26-22:35 UT the eastward expanding auroral (EEA) structures appeared in a sequence such that each new patch formed a little to the east of the previous one. These patches have the same signature as the azimuthally-spaced auroral forms (AAFs) reported by *Elphinstone et al.* (1995) and the EEAS (the eastward-expanding auroral surges) reported by *Tanaka et al.* (2015). Such intensified auroral patches were presumably associated with small-scale upward FAC structures in the postmidnight sector and usually observed after onset of substorm explosive phase (*Wild and Yeoman*, 2000).

The EEA structures originate an undulation of the poleward border of the diffuse aurora, which observed usually during the omega bands in the post-midnight sector of the auroral zone during the recovery phase of a substorm (*Liang et al.,* 2005; *Tanaka et al.,* 2015). Note, that North-South-aligned auroras and pulsating aurora were observed in the diffuse aurora after the passage of the EEA structures in our event after 22:27:40 UT.

Besides, at ~22:26 UT in addition to bright EEA structures, the discrete auroral structures appear from the west along the higher latitude (69°), which also northward and eastward expanded as in cases reported by (*Connors and Rostoker,* 1993, *Opgenoorth et al.*, 1994, *Connors et al.,* 2003).

During this activation A3, the footprints of the THD were located westward the Apatity and outside the field of view of Apatity all-sky camera, near equatorial border of the pulsating diffuse auroras.
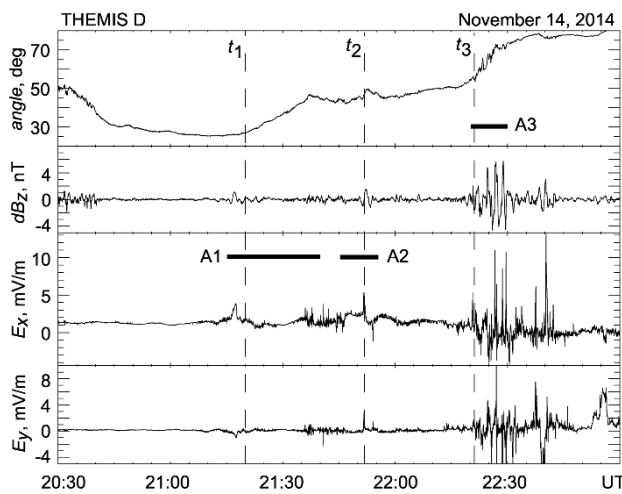
Figure 3. THD satellite data of magnetic and electric fields on Nov 14, 2014 (details in text).

2. Magnetospheric observations

2.1 Particle fluxes and fields. Fig. 3 shows the magnetic and electric fields evolution at THD at the interval 20:30 – 23:00 UT from top to bottom: i) inclination angle of the magnetic field relative to the *XY* plane; ii) *Pi2*-like fluctuations of the magnetic field calculated as the deviations of observed magnetic field from 108-seconds smoothed values, the most appreciable dBz component of the magnetic field is shown here; iii)-iv) E_x and E_y components of the electric field.

From Fig. 3 one can see, that the times of auroral activity enhancement coincide with the times of large-scale dipolarizations of the magnetic field, the increased dB_z pulsations in the *Pi2* range and the enhancement of electric field fluctuations.

Before ~21:15 UT, the inclination angle of the magnetic field decreases in an association with a decline of previous substorm at AMD. After this moment, weak activations A1 and A2 were accompanied by the slow large-scale dipolarization in the magnetosphere at 7.6-8.5 Re. More intense activation A3 occurs, when the THD observed the final sharp large-scale dipolarization in the magnetosphere at ~7.2 Re, when the THD footprint was located near equatorward edge of diffuse aurora.

2.2 Wave activation. Fig. 4 presents the THD observations of the particle flux and the waves (from top to bottom): i) FBK wave data for electric and magnetic fields; ii) total magnetic field; iii) electrons registered by ESA and SST detectors (< 30 keV and > 30 keV); iv) three components of plasma flows. Two bottom panels present two magnetograms from LOZ and AND.

Fig. 4 shows that all three activations A1-A3 are characterized also by the variations of plasma flow velocity with periods which decrease from ~10 min during A1 to ~ 2 min during A3 (Fig. 4). As a whole, it can be seen that the values of azimuthal velocity (v_{yi} >0 - westward) were higher than the plasma velocity in the radial direction ($v_{xi} > 0$ - Earthward). But during A3, the plasma velocity burst ($v_{xi} \sim -80$ km/s) in the tailward radial direction ($v_{xi} < 0$) was observed near the moment t_3, when the poleward auroral boundary expanded to the north.

The character of the energetic electron injections registered during the activations A1-A3 was different. During the A1 and A2, the <100 keV electron injections were observed with the energy-time dispersion. The more energetic (>100 keV) electron injection appears without dispersion during the A3, what can suggest that this injection without dispersion was located near a particle injection source.

During the activation A3, when the footprints of THD were located within pulsating diffuse auroral region, the low-energy electron flux (0.1-3 keV) bursts were observed by the THD. These bursts have the quasi-period ~ 60-90 s and occur at the moments of small-scale local dipolarizations, simultaneously with the enhanced ELF wave bursts at frequencies below 100 Hz observed by THD.
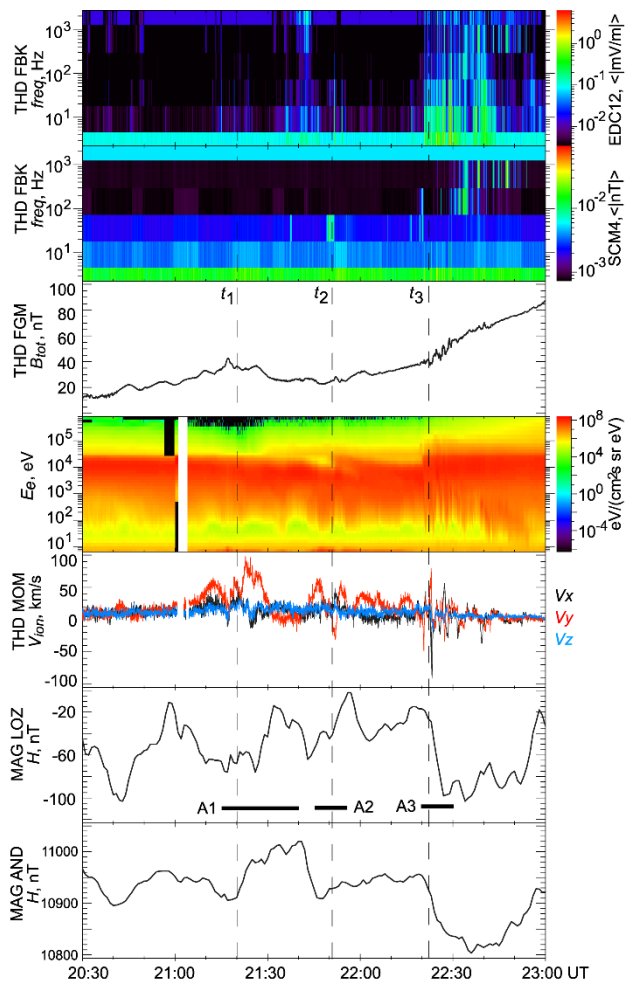
The wave features are more visible in the electric field data. The electrostatic cyclotron harmonic (ECH) waves are observed as discrete intensity enhancements at ~10-200 Hz. The electric field wave power tends to increase during the activity A3, when the auroral intensity is large. The discrete intensity ECH enhancements coincided with the DC electric field variation (the details are not shown).

Figure 4. Wave activity in *B* and *E* fields and particle spectrograms at THD and ground-based magnetograms at LOZ and AND in the interval 20:30-22:40 UT on Nov 14, 2014.

Nishimura et al. (2011) have demonstrated correlation between the pulsating auroral intensity and lower-band chorus intensity observed by the satellite at the equatorial plane of the magnetosphere at 5–9 Re. However in our event the correspondence between whistler wave activity observed by the THEMIS satellite at 6.5–9.25 Re and pulsation is insignificant.

3. Discussion

The EEA structures, observed in our event during A3 in the midnight sector, showed similar properties to the omega bands. However, there are some differences. EEA structures were observed in the midnight sector just after *Pi*2 pulsations onset during substorm activation whereas omega bands are usually observed during the substorm recovery phase in the morning sector. Besides, the EEA structures show strong pulsations in the *X* component, which would be somewhat unusual for omega bands. Although the direct coincidence between the EEA structures and the omega bands was not found, one can suggest that these phenomena may have the same source mechanism in the near-Earth plasma sheet in the end of substorm expansion phase.

Kawasaki and Rostoker (1979) have modeled the eastward propagating disturbance by a three-dimensional current system of narrow longitudinal extent (Cowling channel) in which antiparallel Birkeland current sheets are linked by southward flowing current. Downward flowing FAC located on the poleward side and upward flowing FAC on the equatorward side of the channel. In this model, the electric field is assumed to be uniform, but the conductance is enhanced inside the Cowling channel.

4. Conclusion

The formation of plasma vortices in the magnetosphere during the omega band is usually explained by two models, i.e., bursty bulk flows (BBF) (*Nishimura et al.*, 2011) and the Kelvin–Helmholtz instability arising in sheared flows in the equatorial regions of the tail (*Rostoker and Samson*, 1984). We suggest that the omega-like (EEA) structures observed at ~7.2 Re during the substorm on 14 November 2014 are consistent with the results of Kelvin – Helmholtz type instability near the poleward boundary of the auroral oval at midnight sector of magnetosphere.

References

Connors M. and G. Rostoker (1993) Source mechanisms for morning auroral features. *Geophys. Res. Lett*. V. 20, N. 15. P.1535-1538.

Connors et al. (2003) Ps6 disturbances: relation to substorms and the auroral oval. Ann Geophys. V.21, P.493.

Elphinstone R. D. et al. (1995) Observations in the vicinity of substorm onset: implications for the substorm process. *J. Geophys. Res*. V.100, A5. P. 7939-7969.

Kawasaki K. and G. Rostoker (1979) Perturbation magnetic fielgs and current systems associated with eastward drifting auroral structures. *J. Geophys. Res*. V.88, A4, P. 1464-1480.

Liang J, et al. (2005) Substorm dynamics revealed by ground observations of two-dimensional auroral structures on 9 October 2000. *Ann. Geophys*., V23, P. 3599-3613.

Nishimura Y. et al. (2011) Relations between multiple auroral streamers, pre-onset thin arc formation, and substorm auroral onset. *J. Geophys. Res*., V116, doi: 10.1029/2011JA016768.

Opgenoorth H. J. Persson M. A. L., Pulkkinen T. I., Pellinen R. J. (1994) Recovery phase of magnetospheric substorms and its association with morning-sector aurora. *J. Geophys. Res*., V. 99, N. A3. P.4115-4129.

Rostoker G. and Samson J.C. (1984) Can substorm expansive phase effects arid low frequency Pc magnetic pulsations be attributed to the same source mechanism? *Geophys. Res. Lett*, V.11, P. 271.

Tanaka et al. (2015) Eastward-expanding auroral surges observed in the post-midnight sector during a multiple-onset substorm. *Earth, Planets and Space*, doi: 10.1186/s40623-015-0350-8.

Wild J.A., and T.K. Yeoman (2000) CUTLASS HF radar observations of high-latitude azimuthally propagating vortical currents in the nightside ionosphere during magnetospheric substorms. *Ann. Geophys*., V.18, P. 640-652.